catalysts

MDPI

Article

Enzymatic Polymerization of Dihydroquercetin (Taxifolin) in Betaine-Based Deep Eutectic Solvent and Product Characterization

Maria Khlupova [1], Irina Vasil'eva [1], Galina Shumakovich [1], Elena Zaitseva [2], Vyacheslav Chertkov [2], Alla Shestakova [3], Olga Morozova [1] and Alexander Yaropolov [1,*]

[1] Research Center of Biotechnology of the Russian Academy of Sciences, A. N. Bach Institute of Biochemistry, Leninsky Ave. 33, bld. 2, 119071 Moscow, Russia; dave80@yandex.ru (M.K.); ir-vas@yandex.ru (I.V.); shumakovich1945@yandex.ru (G.S.); morozova@inbi.ras.ru (O.M.)

[2] Department of Chemistry, Lomonosov Moscow State University, Leninskie Gory 1/3, 119991 Moscow, Russia; ezaitseva2008@gmail.com (E.Z.); vchertkov@hotmail.com (V.C.)

[3] State Research Institute of Chemistry and Technology of Organoelement Compounds, Shosse Entuziastov 38, 111123 Moscow, Russia; alshestakova@yandex.ru

* Correspondence: yaropolov@inbi.ras.ru or alexander-yaropolov52@yandex.ru; Tel.: +7-(495)-9544477

Abstract: Deep eutectic solvents (DESs) are an alternative to conventional organic solvents in various biocatalytic reactions. Meanwhile, there have been few studies reporting on synthetic reactions in DESs or DES-containing mixtures involving oxidoreductases. In this work, we have studied the effects of several DESs based on betaine as the acceptor of hydrogen bonds on the catalytic activity and stability of laccase from the basidial fungus *Trametes hirsuta* and performed enzymatic polymerization of the flavonoid dihydroquercetin (DHQ, taxifolin) in a DES–buffer mixture containing 60 vol.% of betaine-glycerol DES (molar ratio 1:2). The use of the laccase redox mediator TEMPO enabled an increased yield of DHQ oligomers (oligoDHQ), with a number average molecular weight of 1800 g mol^{-1} and a polydispersity index of 1.09. The structure of the synthesized product was studied using different physicochemical methods. NMR spectroscopy showed that oligoDHQ had a linear structure with an average chain length of 6 monomers. A scheme for enzymatic polymerization of DHQ in a DES–buffer mixture was also proposed.

Keywords: biocatalysis; deep eutectic solvents; laccase; dihydroquercetin oligomers; NMR

Citation: Khlupova, M.; Vasil'eva, I.; Shumakovich, G.; Zaitseva, E.; Chertkov, V.; Shestakova, A.; Morozova, O.; Yaropolov, A. Enzymatic Polymerization of Dihydroquercetin (Taxifolin) in Betaine-Based Deep Eutectic Solvent and Product Characterization. *Catalysts* **2021**, *11*, 639. https://doi.org/10.3390/catal11050639

Academic Editor: Antonio Zuorro

Received: 29 April 2021
Accepted: 14 May 2021
Published: 17 May 2021

1. Introduction

The use of traditional organic solvents is often limited by their toxicity, explosiveness, and negative impacts on the environment. In recent years, there has been a much greater focus on non-toxic, non-volatile, biodegradable, and environmentally friendly solvents to be used in chemical and biological reactions. In the 1990s, research on the replacement of traditional organic solvents was mainly focused on the use of various ionic liquids (ILs) [1–3]. However, the complexity of synthesis, high cost, and toxicity of ILs significantly limit their use in industry [2,4].

In 2004, a new type of solvents named deep eutectic solvents (DESs), whose physicochemical properties are close to those of ILs, was described by Abbott et al. [5]. Typically, DESs are obtained using the thermal mixing procedure with two components, hydrogen bond donors (HBDs) and hydrogen bond acceptors (HBAs), which results in a eutectic phase with a melting point lower than those of the individual components [5–8]. Choline chloride, choline dihydrogen citrate, betaine, and methyltriphenylphosphonium bromide are mainly used as HBAs; urea, glycerol, malonic acid, lactic acid, ethylene glycol, and xylitol are mainly used as HBDs. Many DESs are liquids at room temperature [5–8]. DESs are characterized by low volatility, high thermal stability, conductivity, and low toxicity; additionally, they are biodegradable. Another advantage of DESs over ILs is the ease of preparation and the ability to vary their physicochemical properties depending on the

nature of the HBA or HBD, the molar ratio of the components, and the water content [5–11]. DESs have low (almost zero) vapor pressure and are viscous liquids. The viscosity of DESs can be significantly reduced by raising the temperature or adding a small amount of water (5–20%). The initial expectations for DESs as universal solvents did not prove to be correct, since the most suitable DES should be developed for each specific process [6,7,10,12,13].

In recent years, there has been an increasing interest in the enzymatic synthesis of compounds involving biocatalysts of various types. Research has focused on both the transformation of natural substrates of enzymes and the technogenic compounds, the biocatalytic conversion of which enables the formation of new materials with various useful properties. The use of enzymes in organic synthesis has several benefits: the reactions proceed under "mild" conditions (close to neutral pH values, room temperature, and atmospheric pressure), there is high enantio- and chemoselectivity [14,15], as well as the potential to kinetically control the process. Enzymatic reactions conducted in DESs meet the requirements of sustainable chemistry [16–18]. The literature describes different uses of DESs as co-solvents for the biotransformation of various compounds [16–22].

Of special interest is the use of laccase as a redox catalyst for fine organic synthesis [23–26]. Laccases (*p*-diphenol: oxygen oxidoreductase, EC 1.10.3.2) belong to copper-containing oxidases; they catalyze the single-electron oxidation of organic and inorganic compounds with the concomitant reduction of dioxygen to water [27,28]. The oxidation of aromatic compounds occurs through a radical mechanism with the subsequent combination of intermediates, resulting in the formation of oligomeric or polymeric products [23,29–31]. The substrate specificity of laccases can be expanded using redox mediators (enzyme enhancers). Redox mediators are low molecular weight laccase substrates, the enzymatic oxidation of which leads to the formation of highly reactive intermediates. These intermediates can oxidize the target substrate at a high rate. The use of laccase–mediator systems in various fields has been widely described in the literature [23,31,32]. Redox mediators can also be used in enzymatic reactions in DESs in order to accelerate the reaction and increase the yield of the final product. There are only a few papers describing the effects of various DESs on the activity and stability of laccases [33–35], as well as two studies in which laccase was used in polymerization of the natural polyphenols (+) catechin [36] and aniline [37] in a DES-containing medium.

Natural polyphenols are used as important base materials in enzymatic modification in order to obtain new chemical compounds with high antioxidant, antimutagenic, anticarcinogenic, antiviral, and anti-inflammatory properties [38–42]. Many biological and pharmacological properties of flavonoids and phytoalexins have been long known, but are still actively researched in the search for new biochemical activities. The metabolism of flavonoids has not been well studied; however, there is evidence that the activity of these compounds in the body persists only for several hours. In addition, many flavonoids exhibit both antioxidant and prooxidant activities and generate reactive oxygen species. Unlike low molecular weight polyphenolic compounds, their oligomeric derivatives have improved physiological characteristics and a longer in vivo life [43–45], and do not exhibit a prooxidant effect [46,47]. Khlupova et al. report that dihydroquercetin oligomers exert dose-dependent effects on the viability of cultured human rhabdomyosarcoma cells [48]. Thus, oligomeric derivatives of flavonoids, including DHQ oligomers, are promising for pharmaceutical use.

Dihydroquercetin (DHQ, taxifolin) (Figure 1) belongs to natural flavonoids. Its chemical structure is close to that of quercetin and rutin. According to the published data, DHQ has a wide range of pharmacological effects, exhibiting antioxidant, angioprotective, hepatoprotective, antitumoral, and other properties [49–52]; however, unlike quercetin, it has no genotoxicity [53]. In addition, DHQ has regulatory properties; controls DNA reparation, apoptosis, and mitochondrial biogenesis; and also regulates the activity of various enzymes [54]. However, DHQ, as with most flavonoids, is poorly soluble in aqueous solutions. We suppose that the solubility of DHQ in DES–buffer mixtures should be higher, which enables the substrate loading to be increased in the case of enzymatic

polymerization of DHQ. Additionally, Toledo et al. showed that the laccase from *Trametes versicolor* retains its activity in betaine- and choline-based DESs, and in some DESs the laccase activity increases up to 200% [34]. The highest activity of the bacterial laccase from *Bacillus* HR03 was registered in 20% (*v*/*v*) glycerol/betaine (2:1) [33].

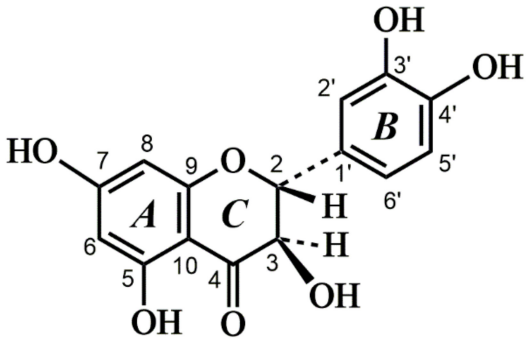

Figure 1. The structural formula and atom numbering of dihydroquercetin.

In this work, we have evaluated the effects of betaine-based DESs and DES–buffer mixtures on the activity and stability of the fungal laccase *Trametes hirsuta*; we have performed biocatalytical polymerization of DHQ in a DES–buffer mixture using the laccase–mediator system and characterized the resulting product using various physicochemical methods.

2. Results and Discussion

As noted earlier, DESs are beneficial solvents for use in various fields, as they are nontoxic, cost-effective, biodegradable, and capable of dissolving large quantities of various substances. When using DESs as a medium for enzymatic reactions, it is necessary to take into account their effects on the activity and stability of the enzyme. Chloride anions are known to inhibit fungal laccases [55]. Therefore, choline chloride as a component of DES greatly impedes the correct assessment of the DES effects on the laccase activity. DESs based on betaine as an acceptor of hydrogen bonds and various donors of hydrogen bonds were used in the work. The compositions and molar ratios of the tested DESs are shown in Table 1. In further experiments, DESs with a HBA/HBD molar ratio of 1:2 were used.

Table 1. Compositions, molar ratios, and temperature at the eutectic point for the tested DESs.

DES Components		Legend	HBA/HBD Molar Ratio	Temperature, °C	Aggregate State at Room Temperature
HBA	HBD				
Betaine, B	Lactic acid, L	B-L (1:1)	1:1	60	Solid
		B-L (1:2)	1:2	40	Clear liquid
		B-L (1:3)	1:3	60	Clear liquid
Betaine, B	Glycerol, G	B-G (1:1)	1:1	60	Solid
		B-G (1:2)	1:2	60	Highly viscous clear liquid
Betaine, B	Propionic acid, P	B-P (1:1)	1:1	40	Solid
		B-P (1:2)	1:2	40	Clear liquid
		B-P (1:3)	1:3	40	Clear liquid

The laccase stability was studied in DESs and DES–buffer mixtures with different volume ratios for the components. In DESs, the enzyme completely lost its activity within 10–180 min (Figure 2), while in certain DES–buffer mixtures, oxidoreductases can retain and even enhance their activity and stability [33–35,56]. Furthermore, the addition of water causes a drastic decrease in the viscosity of DESs, which approaches the viscosity of water [9,57].

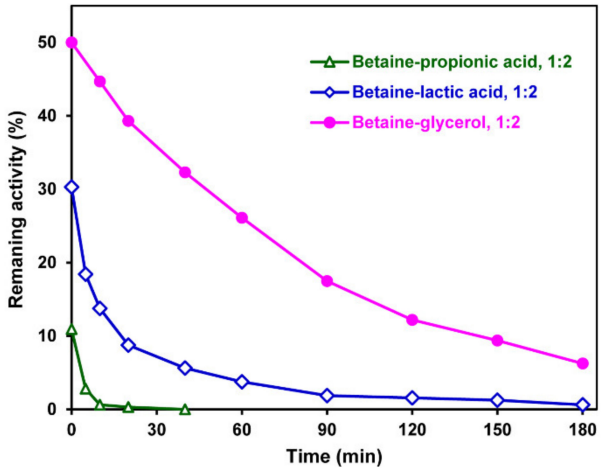

Figure 2. Laccase stability in DESs at room temperature (21–22 °C). Laccase activity in the buffer was considered to be 100%.

In our experiments, the effect of the viscosity of DES–buffer mixtures on the enzyme activity was not taken into account. The study of the stability of laccase at room temperature in B-L(1:2)–buffer and B-P (1:2)–buffer mixtures with different volume ratios of the components has shown that the enzyme completely loses its activity within 4 h (Figure S1). A smooth fall of laccase activity was observed in B-G (1:2)–buffer mixtures, and after 7 days, 47–60% of the enzymes' initial activity remains, depending on the DES volume content in the DES–buffer mixture (Figure 3). Additionally, at DES contents of 10 and 20 vol.%, the laccase activity increased up to 140 and 130%, respectively, in the initial timeframe, which is consistent with the results reported in [34].

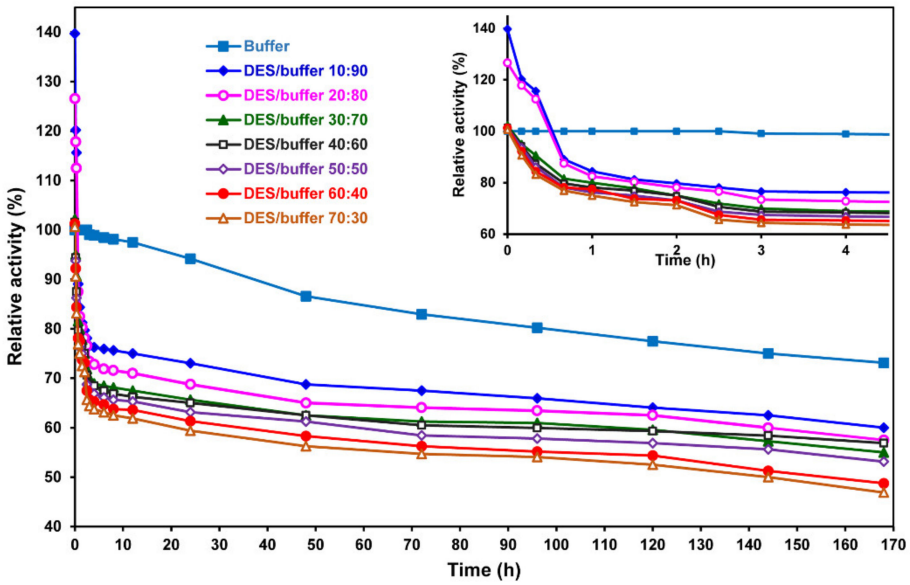

Figure 3. Laccase stability in B-G (1:2)–buffer mixtures with different volume ratios for the components at room temperature (21–22 °C). Laccase activity in the buffer at the initial time was considered to be 100%.

Hammond et al. showed that DES retains up to ~42 wt.% of water in the DES–buffer mixture, and in the case of the higher water content, the DES–buffer mixture should be considered as an aqueous solution of DES components [58]. Therefore, laccase-catalyzed DHQ polymerization was performed in the B-G (1:2)–buffer mixture with a volume ratio of 60:40, at which the weight content of water was ~35%. The use of this mixture enabled a high loading of DHQ (>17 mM), and the enzyme was stable and catalytically active for

12 h of the reaction. In addition, at this component ratio, the reaction mixture had low viscosity, which had no significant impact on the mass transfer of the reagents during the biocatalytic reaction. In order to accelerate the polymerization of DHQ and increase the final product yield, the laccase–mediator system was used. The redox mediator was TEMPO (0.61 mol.% in the reaction mixture). The oligoDHQ yield was 58 ± 7%. (It should be noted that in the case of the laccase-catalyzed polymerization of DHQ in the absence of TEMPO, the oligoDHQ yield was 15 ± 6%.) The gel permeation chromatography data show that oligoDHQ has a number average molecular weight (M_n) of 1800 g mol^{-1} and a polydispersity index (PDI) of 1.09.

The product of the DHQ biocatalytic polymerization was characterized using various methods. The UV-visible spectra for DHQ and oligoDHQ in DMSO are shown in Figure 4a. The DHQ monomer had an intense absorption band at 290 nm. In comparison with the monomer, a long-wave "tail" (305–550 nm) with a pronounced shoulder in the region of 320–350 nm appeared in the oligoDHQ spectrum. The study of DHQ and oligoDHQ by Fourier transform IR spectroscopy (Figure 4b) showed that their spectra are quite similar. The characteristic bands of DHQ are as follows: 3400 cm^{-1} (O–H stretching vibration), 1645 cm^{-1} (C=O stretching in flavones), 1360 cm^{-1} (O–H bending and C–O stretching in phenolic compound), 1264 cm^{-1} (C–O–C stretching in the aryl ether ring ***C***), and 1165 cm^{-1} (characteristic band of 5,7-dihydroxysubstituted flavonoids) [59–61]. At the same time, the absorption bands in the oligoDHQ spectrum are broader and smoother in comparison to the monomer spectrum, and the peaks corresponding to stretching vibrations of phenol groups (1135 and 1115 cm^{-1}) [62] are noticeably lower.

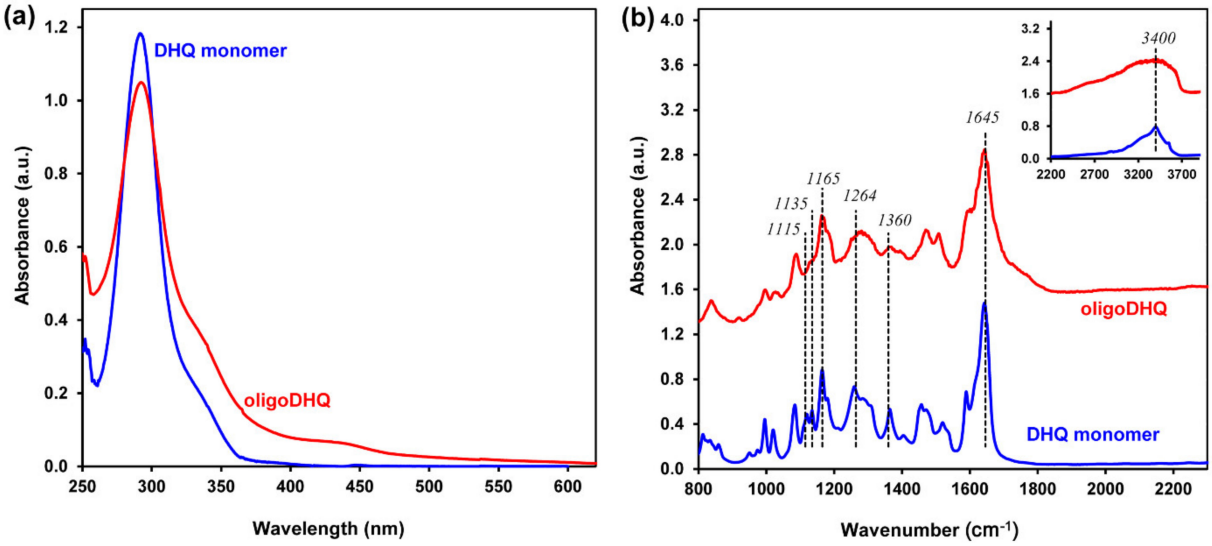

Figure 4. UV-Vis (**a**) and FTIR (**b**) spectra of the DHQ monomer and oligoDHQ.

The type of binding of the monomer units in the polymer chain of the enzymatically synthesized oligoDHQ was determined via ^{1}H and ^{13}C NMR spectroscopy (Figures 5 and 6). Comparative analysis of ^{1}H and ^{13}C spectra of oligoDHQ and DHQ monomer shows that all the peak groups in the oligoDHQ spectra are fairly close to the signals of the monomer.

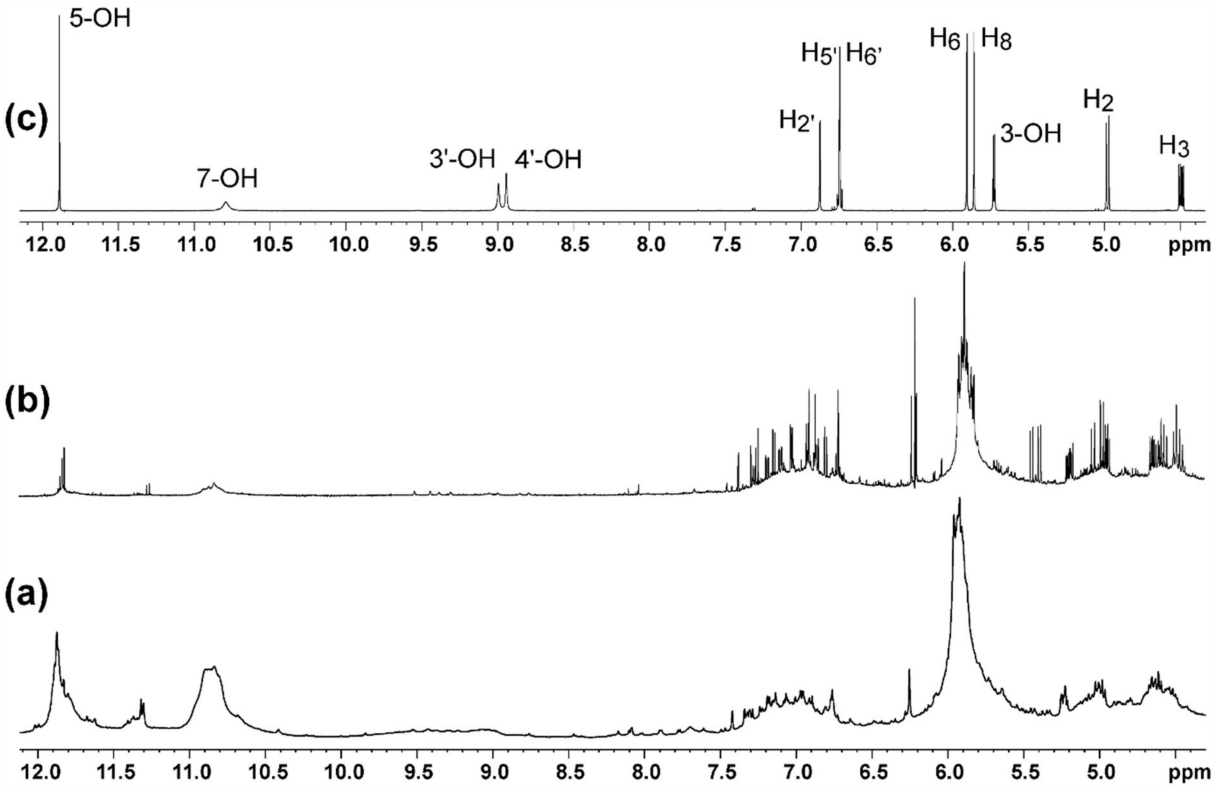

Figure 5. ^{1}H NMR spectra of (**a**) oligoDHQ, (**b**) D_2O-pretreated oligoDHQ, and (**c**) DHQ monomer.

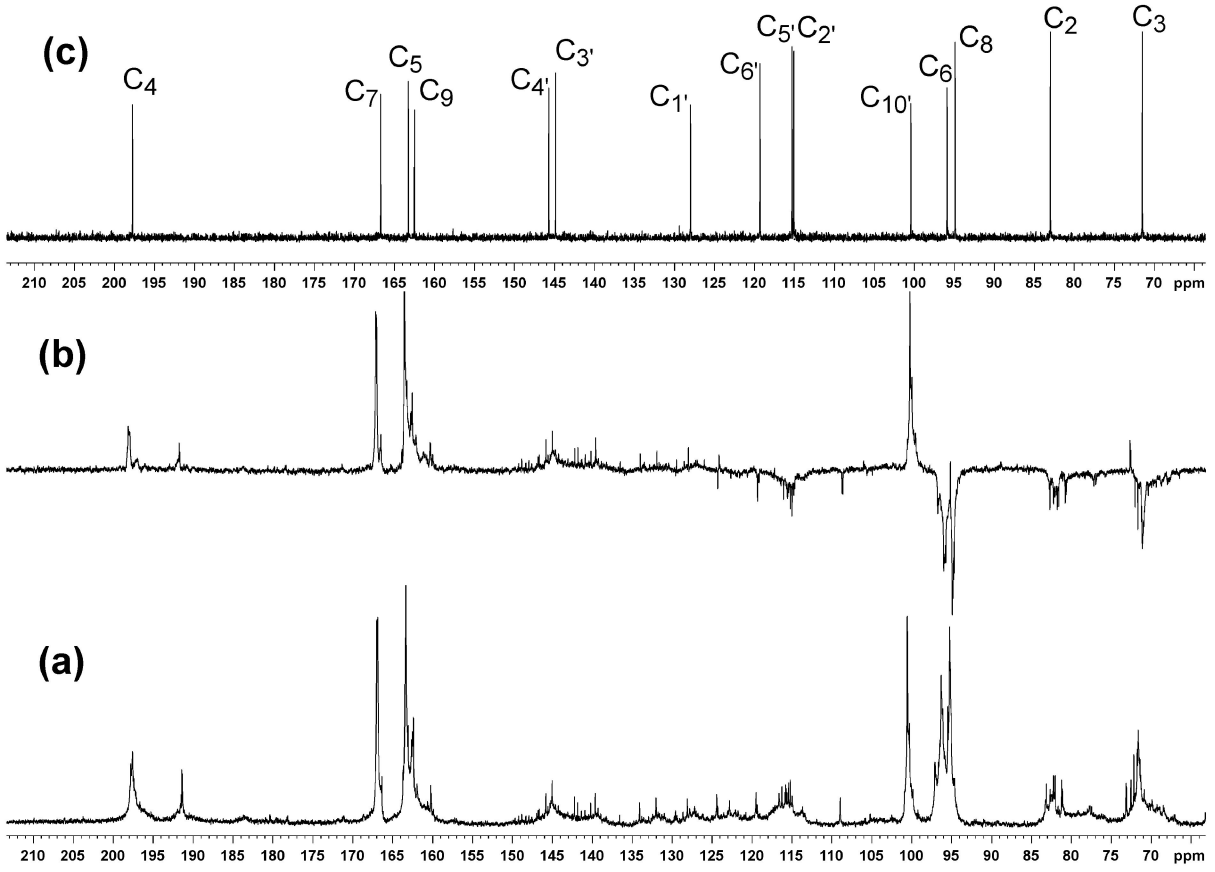

Figure 6. NMR spectra: (**a**) ^{13}C-{^{1}H} of oligoDHQ; (**b**) ^{13}C-APT of oligoDHQ (signals of quaternary C atoms point upwards, signals of CH groups point downwards); (**c**) ^{13}C-{^{1}H} of DHQ monomer.

The ^{1}H NMR spectrum of oligoDHQ (Figure 5a) shows a strong broadening effect on hydroxyl protons (from 8.5 to 12.2 ppm) and complex broadened multiplets in three spectral regions (6.7–7.4, 5.6–6.2, and 4.5–5.5 ppm), which correspond to the DHQ protons H2′, H5′, and H6′ (ring ***B***); H6 and H8 (ring ***A***); and H2 and H3 (ring ***C***), respectively. The numbering of DHQ atoms is shown in Figure 1. The integral intensities of these three regions have approximately the same relative values, although it could be expected that the three protons of ring ***B*** should have a total integral abundance 1.5-fold those of protons of rings ***A*** and ***C***, as occurs for the DHQ monomer. Additionally, it should be noted that the total integral of the hydroxyl protons 3′–OH and 4′–OH (8.2–10.3 ppm) in the oligoDHQ proton spectrum is significantly underestimated (about 30–40%). It follows that the carbon skeleton (rings ***A***, ***B***, and ***C***) of the initial monomer is retained in the course of enzymatic oligomerization, while one of the aromatic protons in ring ***B*** is replaced by an aryloxy or alkoxy radical formed as a result of enzymatic oxidation of DHQ.

In order to simplify the multiplet structure of ^{1}H NMR spectra, an oligoDHQ sample was treated with D_2O to replace protons of hydroxyl groups with deuterium. This allowed us to lower the intensity of hydroxyl peaks by at least an order of magnitude, giving a much better resolved multiplet structure for protons attached to carbons (Figure 5b). Therefore, in the areas of 6.7–7.4 and 4.5–5.5 ppm against the background of very wide signals, multiplets with a well-defined structure and narrow lines appeared. It should be noted that the monomer units in the polymer structure have their own individual characteristics. Monomeric units in the central part of the polymer chain have lower mobility than terminal ones. Because of this, they come out differently in NMR spectra [63]. As a rule, central links that are poorly mobile on the NMR timescale have strongly broadened signals. Terminal blocks, on the contrary, have higher mobility, with well-resolved multiplets correspond to these blocks, allowing one to obtain rich information about the structure. Therefore, we assume that the groups of wide signals correspond to the internal links of oligoDHQ and that the narrow lines correspond to the terminal or peripheral groups of the molecule. For multiplets in the ranges of both 6.7–7.4 and 4.5–5.5 ppm, the total integrated intensity of the narrow-line multiplets is approximately 20% of the intensity of the corresponding wide component.

A comparative analysis of the ^{13}C NMR spectra of oligoDHQ and DHQ monomer (Figure 6) gives basic information about the structure of the oligoDHQ formed during enzymatic polymerization.

First of all, it should be noted that all of the signals of the carbon atoms of ring ***A*** of the monomer correspond to the broadened intense signals in the oligoDHQ spectrum, while the difference in the chemical shifts is not more than 0.4 ppm. When a proton in a benzene ring is replaced by an aryloxy or alkoxy group, the chemical shifts of all the carbon atoms in the ring should change markedly (till 10 ppm). However, this does not apply to the carbon atoms of ring ***A***. The carbon signals C2 and C3 in the oligoDHQ spectrum are groups of narrow signals above the background signals of broadened components, while the entire set of C3 signals occupies a more compact spectrum range than C2 signals. Apparently, more factors affect the change in the chemical shifts of C2 than in C3, since structural changes in ring ***B*** have a stronger effect on the chemical shift of C2.

At the same time, all of the signals of ring ***B*** comprise a set of relatively narrow signals against a background of wide components that are evenly distributed over the entire range of their "own" range of the spectrum. The only exception is the very low-intensity narrow signal of the carbon C6′ at 119.5 ppm, which does not have a corresponding wide component. At the same time, in the region of 125–145 ppm, many new quaternary carbon signals appear. The above indicates that the 6′-position of ring ***B*** is the point of connection during polymerization, i.e., the chain grows due to aryloxy or alkoxy group substitution exclusively in the 6′ position of ring ***B***.

As for the hydroxyl groups involved in the polymerization process, only four groups can participate in the process, and according to our estimates, with close probabilities. Hydroxyl 5–OH participates in a very strong hydrogen bond with carbonyl (hydrogen

bond energy of about 4 kcal mol^{-1}) and cannot compete with the mobile hydroxyls 3–OH, 3′–OH, 4′–OH, and 7–OH. The fact that 5–OH hydroxyl is not involved in the process during polymerization is confirmed by the nature of the signals in the low-field part of the ^{13}C NMR spectrum. If hydroxyl 5–OH participated in the chain growth, then the carbonyl group would have nothing to form a hydrogen bond with, and in this region there should be a characteristic signal at ~210 ppm, which is not observed in the experimental ^{13}C NMR spectrum.

Of interest is the group of several relatively weakly intense quaternary carbon peaks in the range of 191–192 ppm shifted to a strong field relative to the main signal of C4 (at 197 ppm). These peaks also belong to C4 carbon, however they are located in those oligoDHQ units, which contain an aryloxy group at C3 (see reference data on chemical shifts in [64]). Their relative intensity is approximately 15–20% of the intensity of all C4 peaks. This indicates that the alkoxyl radical, which is formed in enzymatic oxidation of DHQ, takes part in DHQ polymerization along with aromatic DHQ radicals.

Additional information about the oligoDHQ structure can be obtained by elucidating the narrowband multiplets of rings ***B*** and ***C***. For this purpose, a two-dimensional NMR spectrum COSY (correlation spectroscopy) was recorded, which allowed us to characterize the structures of local fragments based on characteristic cross-peaks corresponding to intra-ring proton–proton couplings. Two fragments of this spectrum COSY are shown in Figure S2. The elucidation of the cross-peaks of ring ***B*** (Figure S2a) and multiplets of the 1D proton NMR spectrum in the region of 6.7–7.4 ppm revealed five spin systems of the ABX type, characteristic of the interaction between *ortho* and *meta* protons of ring ***B*** (H2′, H5′ and H6′), for which the vicinal couplings $^{3}J_{H5'–H6'}$ lie within 8.27–8.36 Hz and the values of four-bond coupling $^{4}J_{H2'–H6'}$ vary from 2.03 to 2.12 Hz (Figure S2a and Table S1). It follows that oligoDHQ includes five fairly mobile benzene rings with a relative arrangement of all three substituents at two oxygen and one carbon atoms (ring ***B***). The variability of these fragments may be due to the structure and conformation of a substituent at one of the oxygen atoms. Via this atom, the terminal fragment is linked to the main chain of the oligomer.

A thorough analysis of multiplets in the region of 4.5–5.5 ppm allowed us to determine nine spin systems of the AX type corresponding to protons H2 and H3 of ring ***C*** from the terminal fragments of oligoDHQ. The vicinal coupling $^{3}J_{H2–H3}$ varies from 10.68 to 12.05 Hz. The values of chemical shifts of proton H2 lie in the range of 4.96–5.48 ppm, and of proton H3 in the range of 4.49–4.68 ppm (Figure S2b and Table S1). These $^{3}J_{H2–H3}$ bond values are typical of the trans-position of H2 and H3 protons in naturally occurring dihydroquercetin. The values of this coupling lie in the range from 11.37 to 12.10 Hz for known derivatives of trans-dihydroquercetin with substituents at the oxygen atom [64]. Thus, the data reported in the present work show that the stereochemistry of the ***C*** ring persists in the course of DHQ oligomerization. For comparison, we note that the values of this type of bond for the analogous cis-isomers known from the literature are in the range of 2.26–3.88 Hz [65].

The presence of such clearly defined multiplets of specific DHQ fragments in the oligoDHQ spectrum suggests with certainty that the stereochemistry of the carbon skeleton of the alkyl chains in the terminal fragments of the ***C*** ring also remain in the course of the DHQ oligomerization. The differences in the values of chemical shifts of these fragments can be attributed to changes in the spatial environment as a result of the attachment of new units to the DHQ molecule via the formation of ether bonds and substitution at C6′.

The intensity of the broadened signals of H6 and H8 in oligoDHQ protons indicate that there are two protons. This confirms the earlier conclusion that ring ***A*** does not undergo a radical attack during enzymatic polymerization under the conditions described in this work.

Based on the literature data, oxidative polymerization of DHQ can be considered as a two-stage process [66]. In the first stage, the DHQ molecule is activated by laccase to form an alkoxy or aryloxy radical [67]. The enzyme can catalyze the oxidation of one of the four

DHQ hydroxyl groups (3–OH, 3′–OH, 4′–OH, or 7–OH). In the second stage, the radical substitution of the hydrogen atom in the aromatic ring occurs with the formation of a new C-O bond. Based on the analysis of ^{1}H and ^{13}C NMR spectra, we have shown that radical substitution predominantly happens at the position C6′ of ring ***B***.

The results of our study contradict the widespread opinion that during electrophilic substitution, which in early works was often treated as radical substitution, an attack occurs at the position with the highest electron density of the aromatic substrate [68]. From this standpoint, the positions of C6 and to a lesser degree of C8 are the priority targets of an electrophilic attack. Indeed, all the three π-donor substituents (5–OH and 7–OH hydroxyl groups and the chromene oxygen of ring ***C***), as well as the π-acceptor carbonyl group, act in concert, and their combined effect should increase the electron density on C6 and C8. Our model calculations (UB3LYP/6-311++G(d,p) [69]) confirm this qualitative conclusion. The calculated charges on C6 and C8 carbon atoms of ring ***A*** have high values of −0.144ē and −0.124ē, respectively, due to the coordinated action of all four substituents on DHQ ring ***A***, while due to the dissonance of the electronic effects of the three donor substituents of ***B*** ring, the absolute values of the charges on the carbon atoms C2′, C5′, and C6′ are significantly lower (−0.095ē, −0.108ē, and −0.087ē, respectively). These data are consistent with the formation of 6- and 8-substituted products in both bromination of DHQ and the Mannich reaction under conditions suitable for classic electrophilic substitution [70,71].

Recently, some important results have appeared that clarify the mechanism of interaction of radicals with aromatic substrates [72]. It has been shown that when there are several competing reaction pathways, a product is formed, the pathway to which goes through a more stable transition state. Boursalian et al. showed that for six-membered aromatic rings, substantial additional stabilization of a reaction's transition state could be provided by electron-donating substituents located in the *para*-position of the reaction center [72].

The idea that radical substitution predominantly functionalizes the C–H bond in the *para*-position to the OH or OR groups has dramatically changed our concept of a possible reaction product. In the DHQ molecule, the additional stabilization factor by the *para*-substituent attached via oxygen is essential only for the C6 carbon of ring ***A*** (due to chromene oxygen O1) and the C6′ carbon of ring ***B*** (due to the 3′–OH group).

We performed a series of quantum mechanical model calculations of DHQ transition state structures during a radical attack at the C6 and C6′ positions. For this, hydroxyl, methoxyl, and phenoxyl radicals were used as attacking particles. The calculations were performed taking into account open shells in the UB3LYP/6-311++G(d, p) approximation [69]. The stationary stable transition state structures under the action of each of the three radicals on ring ***A*** and ring ***B*** of DHQ are shown in Figure 7.

In all three cases, much lower activation energy is required to achieve the transition state when attacking carbon C6′ of ring ***B*** than when attacking carbon C6 of ring ***A***. The difference is maximal for R = OH (ΔE = 3.8 kcal mol^{-1}) and somewhat lower for R = OMe (ΔE = 2.4 kcal mol^{-1}) and OPh (ΔE = 2.8 kcal mol^{-1}). Our NBO analysis of transition states for a radical attack on carbon C6 of ring ***A*** shows that its electron structure is strongly affected by two factors: the formation of a strong hydrogen bond between the 5–OH group and carbonyl oxygen and conjugation of the carbonyl group with chromene oxygen. Both of these effects lower the order of the C5–C10 bond (Figure 7b), and as a result weaken the efficiency of stabilization of the radical transition state due to chromene oxygen O1. On the contrary, a radical attack at the C6′ position results in complete stabilization of the transition state from the hydroxyl 3′–OH via the *para*-quinoid structure with full C1′–C2′ and C4′–C5′ double bonds. These calculations support our experimental results. Interestingly, the heterocoupling of DHQ and *p*-aminobenzoic acid in the laccase-catalyzed reaction also occurs at position C6′ of ring ***B*** [48].

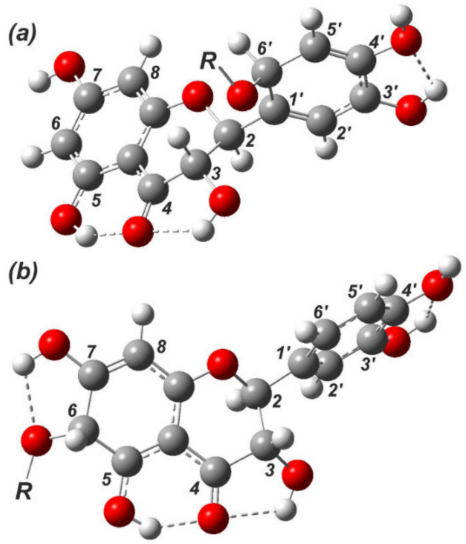

Figure 7. Spatial structure of the transition states for a radical attack on (**a**) carbon C6′ of ring ***B*** and (**b**) carbon C6 of ring ***A***, modeled for ***R*** = H, Me, and Ph.

Therefore, a comparative analysis of the ^{1}H and ^{13}C NMR spectra of the monomer and oligoDHQ allows us to draw the following conclusions. Enzymatic polymerization causes no change in the carbon skeleton of DHQ or the stereochemistry of the C2–C3 fragment. The C6′ position is the only position to be substituted in the aromatic ring, which means that the structure of the oligoDHQ backbone is predominantly unbranched. The binding of DHQ units occurs randomly; the oligomer chain grows when an active radical, which is formed equally likely from any of four hydroxyl groups (excluding 5–OH), attacks C6′ of ring ***B***. As a result, the oligomer with a small number of units is formed. The average length of the oligomer chain is six DHQ units according to NMR spectroscopy. Hence, laccase-catalyzed DHQ oligomerization in the DES–buffer mixture is a regio- and stereospecific biotransformation.

Based on the data obtained, we propose a scheme for DHQ enzymatic polymerization in a DES–buffer mixture using the laccase–mediator system (Figure 8).

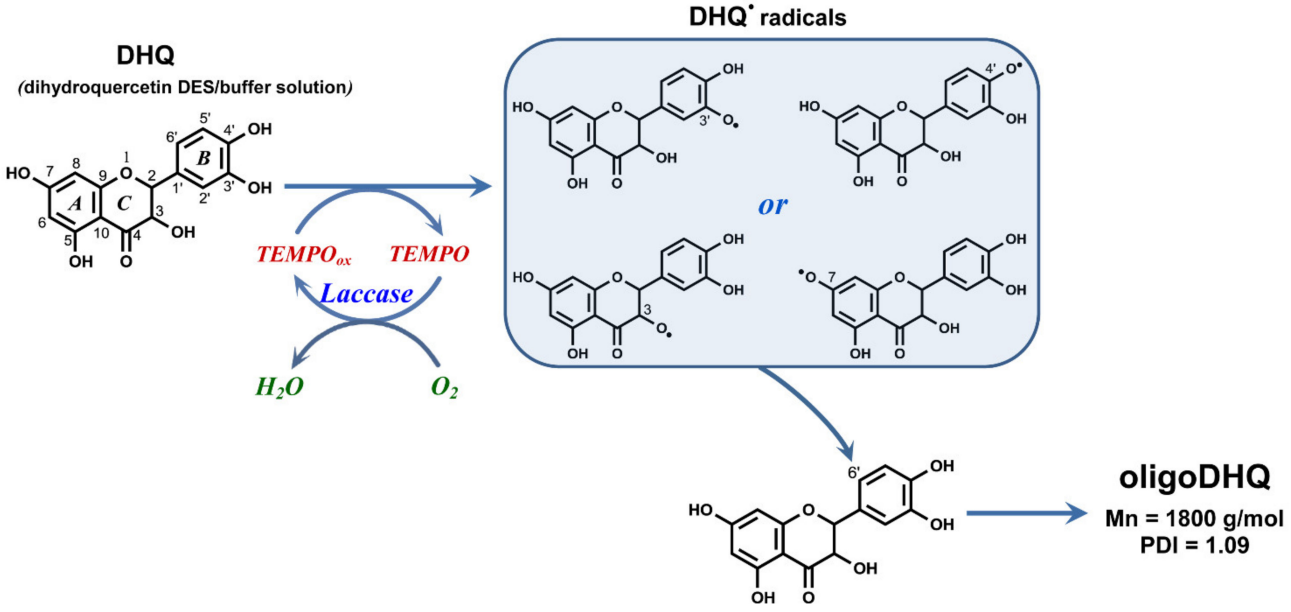

Figure 8. Schematic illustration of DHQ polymerization using the laccase-TEMPO system.

3. Materials and Methods

3.1. Materials

All commercially available chemicals were of high purity and were used without further purification, namely KH_2PO_4, NaOH, citric acid, 2,2′-azino-bis(3-ethylbenzothiazoline-6-sulfonic acid) diammonium salt (ABTS), tetrahydrofurane (THF), (2,2,6,6-tetramethylpiperidine-1-oxyl) (TEMPO), betaine (Sigma-Aldrich, Saint Louis, MO, USA), DMSO-D_6 (Aldrich), dimethylsulfoxide (DMSO, Marbiopharm, Yoshkar-Ola city, Russia), glycerol 99% (Panreac Quimica SA, Barselona, Spain), propionic acid 99% (Carl Roth GmbH, Karlsruhe, Germany), and lactic acid 90% (Acros Organics, Geel, Belgium). Dihydroquercetin (≥96%) was purchased from BioChemMak-ST, Moscow, Russia. All of the solutions were prepared using water purified with a Simplicity® Water Purification System (Merck KGaA, Darmstadt, Germany).

3.2. Enzyme

A laccase from the fungus *Trametes hirsuta* (Wulfen) Pilát CF-28 was purified to homogeneity as described previously [73]. The laccase activity was measured spectrophotometrically using 1 mM ABTS as a chromogenic substrate (λ = 420 nm, ε = 36,000 $M^{-1}cm^{-1}$) at 24 °C in 0.1 M Na-citrate-phosphate buffer at pH 4.5. One unit of activity is defined as the amount of laccase oxidizing 1 μM of substrate per min. The specific activity of the enzyme stock solution was about 148 U/mg of protein. The protein concentration was determined as described in [74] by the difference in the optical density of the protein solution at 228.5 and 234.5 nm using a bovine serum albumin (BSA) as standard. The protein concentration was ca. 7.8 mg mL^{-1}.

3.3. Preparation of DESs and DES–Buffer Mixtures

All DESs: betaine/lactic acid (B-L, molar ratio 1:1; 1:2; 1:3), betaine/propionic acid (B-P, molar ratio 1:1; 1:2; 1:3), and betaine/glycerol (B-G, molar ratio 1:1; 1:2) were obtained using a thermal mixing procedure. DES–buffer binary mixtures were obtained by adding various volumes of DES to 0.1 M phosphate buffer (pH 6.5).

3.4. Determination of the Activity and Stability of Laccase in DESs and DES–Buffer Mixture

To study the enzyme stability in DESs and DES–buffer mixtures, a laccase stock solution was previously diluted 3 times with 0.1 M phosphate buffer (pH 6.5). Then, 100 μL of the diluted laccase solution was added to 2.5 mL of DESs or DES–buffer and mixed vigorously. Next, 50 μL samples were taken at regular intervals and added to 1 mL of 0.1 M phosphate buffer (pH 6.5), and the resultant solution was taken for the laccase activity assay. The enzymatic reaction was initiated at 24 °C by adding a 50 μL sample to 2.5 mL of 1 mM ABTS in 0.1 M Na-citrate-phosphate buffer at pH 4.5. All experiments were performed in triplicate and the maximum relative measurement error was about 3.56%.

3.5. Enzymatic Polymerization of DHQ in DES–Buffer Mixture

The enzymatic synthesis of DHQ oligomers was carried out in a mixture of DES B-G (molar ratio 1:2) (60 vol.%) and 0.1 M Na-citrate-phosphate buffer (pH 4.5). In a typical experiment, 50 mg of DHQ was dissolved in 6 mL of DES. Then, 4 mL of the buffer was added to the resulting solution and mixed. The final concentration of DHQ in the reaction medium was 16.4 mM. Next, 0.156 mg of the TEMPO redox mediator (concentration in the reaction medium of 0.1 mM; 0.61 mol.%) was added and the monomer polymerization was initiated by adding the laccase stock solution. The specific activity of the enzyme in the reaction mixture was ~1.0 U mL^{-1}. The synthesis was performed under aerobic conditions at room temperature (21–22 °C) and with constant stirring on a magnetic stirrer for 12 h. Then, the resultant clear solution was diluted 5 times with deionized water; the oligoDHQ precipitate was separated by centrifugation, repeatedly washed with a 3 vol.% ethanol solution in order to remove low molecular weight compounds, dried to constant weight, and used in further experiments. The product yield was calculated as the ratio of the mass

of the obtained oligoDHQ to the mass of the starting monomer. All experiments were performed in triplicate.

3.6. Characterization of DHQ Polymerization Product

The number average molecular weight (M_n) and the polydispersity index (PDI) of the enzymatically synthesized oligoDHQ were determined by gel exclusion chromatography using an RI detector. The determination was carried out on a Styragel HR 1E 300 × 7.8 mm column (Waters, Milford, MA, USA) using THF as the mobile phase. The column was calibrated by polysterene standards. The concentration of the samples was 1 mg mL^{-1}; the volume of the injected sample was 30 µL.

UV-visible spectra of oligoDHQ were recorded using a Shimadzu UV1240 mini spectrophotometer (Shimadzu Europa GmbH, Duisburg, Germany). FTIR spectra were recorded using KBr pellets on a Frontier FT IR/FIR spectrometer (PerkinElmer Inc., Waltham, MA, USA).

^1H, ^{13}C, and ^{13}C-APT NMR spectra and the two-dimensional COSY oligoDHQ spectrum were recorded in DMSO-D_6 at 303 K using a Bruker AVANCE 600 spectrometer with an operating frequency of 600.03 MHz for ^1H nuclei with the parameters given in [75]. The deuterated oligoDHQ preparation was obtained by treating oligoDHQ with heavy water (D_2O, 99.8% enrichment level). In order to achieve this, a suspension of 25 mg of oligoDHQ was stirred in 2 mL of D_2O for 2 h at room temperature; then, the heavy water was evaporated on a rotary evaporator and the product was finally dried under high vacuum (~5.0×10^{-3} Torr.) After the procedure was repeated twice, the enrichment of hydroxyl groups with deuterium atoms was 90% according to ^1H NMR.

4. Conclusions

The present work demonstrates the possibility of using betaine–glycerol DES as a co-solvent for the effective laccase-catalyzed polymerization of the flavonoid dihydroquercetin (taxifolin). The composition of the reaction medium meets the requirements of sustainable chemistry. The use of a redox mediator of the enzyme can significantly increase the yield of the target oligoDHQ product. OligoDHQ has a number average molecular weight of 1800 g mol^{-1} and a polydispersity index of 1.09. The structure of the synthesized product was studied using NMR spectroscopy, and it was shown that oligoDHQ has a linear structure with an average chain length of six monomer units. Since DHQ oligomers can find application in pharmacology, further studies of the biological activity of the oligoDHQ synthesized in the present work are in progress.

Supplementary Materials: The following are available online at https://www.mdpi.com/article/10.3390/catal11050639/s1: Figure S1: Laccase stability in B–L (1:2)–buffer (**a**) and B–P (1:2)–buffer (**b**) mixtures with different component volume ratios. Figure S2: Two-dimensional NMR spectrum COSY of D_2O pretreated oligoDHQ protons (**a**) H2′, H5′, H6′ (ring ***B***); and (**b**) H2, H3 (ring ***C***). Table S1: Parameters of the ^1H NMR spectra of the terminal fragments of oligoDHQ: chemical shifts (δ_H, ppm), spin–spin coupling constants $^nJ_{HH}$ (Hz).

Author Contributions: A.Y., E.Z. and V.C. conceived and designed the experiments. M.K., G.S. and I.V. performed biochemical experiments. A.S. and V.C. performed all NMR experiments. A.Y. and O.M. analyzed the data and designed and wrote the paper. All authors have read and agreed to the published version of the manuscript.

Funding: The reported study was partially supported by the Russian Foundation for Basic Research, project no. 20-08-00104.

Conflicts of Interest: The authors declare no conflict of interest.

References

1. Rogers, R.; Seddon, K. Ionic Liquids—Solvents of the Future? *Science* **2003**, *302*, 792–793. [CrossRef] [PubMed]
2. Plechkova, N.; Seddon, K. Applications of ionic liquids in the chemical industry. *Chem. Soc. Rev.* **2008**, *37*, 123–150. [CrossRef] [PubMed]

3. Vekariya, R. A review of ionic liquids: Applications towards catalytic organic transformations. *J. Mol. Liq.* **2017**, *227*, 44–60. [CrossRef]
4. Wells, A.; Coombe, V. On the Freshwater Ecotoxicity and Biodegradation Properties of Some Common Ionic Liquids. *Org. Process Res. Dev.* **2006**, *41*, 797–828. [CrossRef]
5. Abbott, A.; Boothby, D.; Capper, G.; Davies, D.; Rasheed, R. Deep Eutectic Solvents Formed between Choline Chloride and Carboxylic Acids: Versatile Alternatives to Ionic Liquids. *J. Am. Chem. Soc.* **2004**, *126*, 9142–9147. [CrossRef] [PubMed]
6. Smith, E.; Abbott, A.; Ryder, K. Deep Eutectic Solvents (DESs) and Their Applications. *Chem. Rev.* **2014**, *114*, 11060–11082. [CrossRef] [PubMed]
7. Wazeer, I.; Hayyan, M.; Hadj-Kali, M. Deep eutectic solvents: Designer fluids for chemical processes. *J. Chem. Technol. Biotechnol.* **2018**, *93*, 945–958. [CrossRef]
8. Hansen, B.; Spittle, S.; Chen, B.; Poe, D.; Zhang, Y.; Klein, J.; Horton, A.; Adhikari, L.; Zelovich, T.; Doherty, B.; et al. Deep eutectic solvents: A review of fundamentals and applications. *Chem. Rev.* **2021**, *121*, 1232–1285. [CrossRef] [PubMed]
9. Dai, Y.; Witkamp, G.-J.; Verpoorte, R.; Choi, Y. Tailoring properties of natural deep eutectic solvents with water to facilitate their applications. *Food Chem.* **2015**, *187*, 14–19. [CrossRef] [PubMed]
10. Vanda, H.; Dai, Y.; Wilson, E.; Verpoorte, R.; Choi, Y. Green solvents from ionic liquids and deep eutectic solvents to natural deep eutectic solvents. *C. R. Chim.* **2018**, *21*, 628–638. [CrossRef]
11. Cicco, L.; Dilauro, G.; Perna, F.; Vitale, P.; Capriati, V. Advances in deep eutectic solvents and water: Applications in metal- and biocatalyzed processes, in the synthesis of APIs, and other biologically active compounds. *Org. Biomol. Chem.* **2021**, *19*, 2558–2577. [CrossRef] [PubMed]
12. Tomé, L.; Baião, V.; Silva, W.; Brett, C. Deep eutectic solvents for the production and application of new materials. *Appl. Mater. Today* **2018**, *10*, 30–50. [CrossRef]
13. Mbous, Y.; Hayyan, M.; Hayyan, A.; Wong, W.; Hashim, M.; Looi, C. Applications of deep eutectic solvents in biotechnology and bioengineering—Promises and challenges. *Biotechnol. Adv.* **2017**, *35*, 105–134. [CrossRef] [PubMed]
14. Wescott, C.R.; Klibanov, A.M. The solvent dependence of enzyme specificity. *BBA Protein Struct. M.* **1994**, *1206*, 1–9. [CrossRef]
15. Rasor, J.P.; Voss, E. Enzyme-catalyzed processes in pharmaceutical industry. *Appl. Catal. A Gen.* **2001**, *221*, 145–158. [CrossRef]
16. Juneidi, I.; Hayyan, M.; Hashim, M.A. Intensification of biotransformations using deep eutectic solvents: Overview and outlook. *Process Biochem.* **2018**, *66*, 33–60. [CrossRef]
17. Pätzold, M.; Siebenhaller, S.; Kara, S.; Liese, A.; Syldatk, C.; Holtmann, D. Deep Eutectic Solvents as Efficient Solvents in Biocatalysis. *Trends Biotechnol.* **2019**, *37*, 943–959. [CrossRef]
18. Xu, P.; Zheng, G.W.; Zong, M.H.; Li, N.; Lou, W.Y. Recent progress on deep eutectic solvents in biocatalysis. *Bioresour. Bioprocess.* **2017**, *4*, 34. [CrossRef] [PubMed]
19. Hassani, F.; Amzazi, S.; Lavandera, I. The versatile applications of DES and their influence on oxidoreductase-mediated transformations. *Molecules* **2019**, *24*, 2190–2208. [CrossRef]
20. Gotor-Fernández, V.; Paul, C. Deep eutectic solvents for redox biocatalysis. *J. Biotechnol.* **2019**, *293*, 24–35. [CrossRef]
21. Panić, M.; Bubalo, M.C.; Redovniković, I.R. Designing a biocatalytic process involving deep eutectic solvents. *J. Chem. Technol. Biotechnol.* **2021**, *96*, 14–30. [CrossRef]
22. Erol, Ö.; Hollmann, F. Natural deep eutectic solvents as performance additives for biocatalysis. *Adv. Bot. Res.* **2021**, *97*, 95–132. [CrossRef]
23. Witayakran, S.; Ragauskas, A. Synthetic Applications of Laccase in Green Chemistry. *Adv. Synth. Catal.* **2009**, *351*, 1187–1209. [CrossRef]
24. Bassanini, I.; Ferrandi, E.E.; Riva, S.; Monti, D. Biocatalysis with Laccases: An Updated Overview. *Catalysts* **2021**, *11*, 26. [CrossRef]
25. Romero-Guido, C.; Baez, A.; Torres, E. Dioxygen Activation by Laccases: Green Chemistry for Fine Chemical Synthesis. *Catalysts* **2018**, *8*, 223. [CrossRef]
26. Itoh, T.; Itoh, T. Laccase-catalyzed reactions in ionic liquids for green sustainable chemistry. *ACS Sustain. Chem. Eng.* **2021**, *9*, 1443–1458. [CrossRef]
27. Solomon, E.; Sundaram, U.; Machonkin, T. Multicopper Oxidases and Oxygenases. *Chem. Rev.* **1996**, *96*, 2563–2605. [CrossRef]
28. Morozova, O.V.; Shumakovich, G.P.; Gorbacheva, M.A.; Shleev, S.V.; Yaropolov, A.I. "Blue" Laccases. *Biochemistry* **2007**, *72*, 1136–1150. [CrossRef] [PubMed]
29. Walde, P.; Guo, Z. Enzyme-catalyzed chemical structure-controlling template polymerization. *Soft Matter* **2011**, *7*, 316–331. [CrossRef]
30. Hollmann, F.; Arends, I. Enzyme Initiated Radical Polymerizations. *Polymers* **2012**, *4*, 759–793. [CrossRef]
31. Mogharabi, M.; Faramarzi, M. Laccase and Laccase-Mediated Systems in the Synthesis of Organic Compounds. *Adv. Synth. Catal.* **2014**, *356*, 897–927. [CrossRef]
32. Morozova, O.V.; Shumakovich, G.P.; Shleev, S.V.; Yaropolov, Y.I. Laccase-mediator systems and their applications: A review. *Appl. Biochem. Microbiol.* **2007**, *43*, 523–535. [CrossRef]
33. Khodaverdian, S.; Dabirmanesh, B.; Heydari, A.; Dashtban-moghadam, E.; Khajeh, K.; Ghazic, F. Activity, stability and structure of laccase in betaine based natural deep eutectic solvents. *Int. J. Biol. Macromol.* **2018**, *107*, 2574–2579. [CrossRef] [PubMed]
34. Toledo, M.; Pereira, M.; Freire, M.; Silva, J.; Coutinho, J.; Tavares, A. Laccase Activation in Deep Eutectic Solvents. *ACS Sustain. Chem. Eng.* **2019**, *7*, 11806–11814. [CrossRef]

35. Delorme, A.E.; Andanson, J.M.; Verney, V. Improving laccase thermostability with aqueous natural deep eutectic solvents. *Int. J. Biol. Macromol.* **2020**, *163*, 919–926. [CrossRef]
36. Ünlü, A.; Prasad, B.; Anavekar, K.; Bubenheim, P.; Liese, A. Investigation of a green process for the polymerization of catechin. *Prep. Biochem. Biotechnol.* **2017**, *47*, 918–924. [CrossRef] [PubMed]
37. Altundağ, A.; Ünlü, A.E.; Takaç, S. Deep eutectic solvent-assisted synthesis of polyaniline by laccase enzyme. *J. Chem. Technol. Biotechnol.* **2020**, *96*, 1107–1115. [CrossRef]
38. Jankun, J.; Selman, S.; Swiercz, R.; Skrzypczak-Jankun, E. Why drinking green tea could prevent cancer. *Nature* **1997**, *387*, 561. [CrossRef]
39. Nakagawa, K.; Ninomiya, M.; Okubo, T.; Aoi, N.; Juneja, L.; Kim, M.; Yamanaka, K.; Miyazawa, T. Tea Catechin Supplementation Increases Antioxidant Capacity and Prevents Phospholipid Hydroperoxidation in Plasma of Humans. *J. Agric. Food Chem.* **1999**, *47*, 3967–3973. [CrossRef] [PubMed]
40. Bordoni, A.; Hrelia, S.; Angeloni, C.; Giordano, E.; Guarnieri, C.; Caldarera, C.; Biagi, P. Green tea protection of hypoxia/reoxygenation injury in cultured cardiac cells. *J. Nutr. Biochem.* **2002**, *13*, 103–111. [CrossRef]
41. Zhao, J.; Wang, J.; Chen, Y.; Agarwal, R. Anti-tumor-promoting activity of a polyphenolic fraction isolated from grape seeds in the mouse skin two-stage initiation-promotion protocol and identification of procyanidin B5-3′-gallate as the most effective antioxidant constituent. *Carcinogenesis* **1999**, *20*, 1737–1745. [CrossRef] [PubMed]
42. Nagarajan, S.; Nagarajan, R.; Kumar, J.; Salemme, A.; Togna, A.R.; Saso, L.; Bruno, F. Antioxidant Activity of Synthetic Polymers of Phenolic Compounds. *Polymers* **2020**, *12*, 1646. [CrossRef]
43. Düweler, K.; Rohdewald, P. Urinary metabolites of French maritime pine bark extract in humans. *Pharmazie* **2000**, *55*, 364–368. Available online: https://pubmed.ncbi.nlm.nih.gov/11828617/ (accessed on 30 March 2021). [PubMed]
44. Kurisawa, M.; Chung, J.; Uyama, H.; Kobayashi, S. Enzymatic synthesis and antioxidant properties of poly(rutin). *Biomacromolecules* **2003**, *4*, 1394–1399. [CrossRef] [PubMed]
45. Kurisawa, M.; Chung, J.; Uyama, H.; Kobayashi, S. Laccase-catalyzed synthesis and antioxidant property of poly(catechin). *Macromol. Biosci.* **2003**, *3*, 758–764. [CrossRef]
46. Li, C.; Xie, B. Evaluation of the antioxidant and pro-oxidant effects of tea catechin oxypolymers. *J. Agric. Food Chem.* **2000**, *48*, 6362–6366. [CrossRef]
47. Bruno, F.; Nagarajan, S.; Nagarajan, R.; Kumar, J.; Samuelson, L. Biocatalytic synthesis of water-soluble oligo(catechins). *J. Macromol. Sci. A* **2005**, *42*, 1547–1554. [CrossRef]
48. Khlupova, M.E.; Morozova, O.V.; Vasil'eva, I.S.; Shumakovicha, G.P.; Zaitseva, E.A.; Pashintseva, N.V.; Kovalev, L.I.; Shishkin, S.S.; Chertkov, V.A.; Shestakova, A.K.; et al. Laccase catalyzed heterocoupling of dihydroquercetin and *p*-aminobenzoic acid: Effect of the reaction product on cultured cells. *Biochemistry* **2018**, *83*, 992–1001. [CrossRef]
49. Weidmann, A. Dihydroquercetin: More than just an impurity? *Eur. J. Pharmacol.* **2012**, *684*, 19–26. [CrossRef]
50. Pantouris, G.; Mowat, C. Antitumour agents as inhibitors of tryptophan 2,3-dioxygenase. *Biochem. Biophys. Res. Comm.* **2014**, *443*, 28–31. [CrossRef] [PubMed]
51. Polyak, S.; Morishima, C.; Lohmann, V.; Pal, S.; Lee, D.; Liu, Y.; Graf, T.; Oberlies, N. Identification of hepatoprotective flavonolignans from silymarin. *Proc. Natl. Acad. Sci. USA* **2010**, *107*, 5995–5999. [CrossRef] [PubMed]
52. Sato, M.; Murakami, K.; Uno, M.; Ikubo, H.; Nakagama, Y.; Katayama, S.; Akagi, K.; Irie, K. structure-activity relationship for (+)-taxifolin isolated from silymarin as an inhibitor of amyloid β aggregation. *Biosci. Biotechnol. Biochem.* **2013**, *77*, 1100–1103. [CrossRef]
53. Makena, P.; Pierce, S.; Chung, K.T.; Sinclair, S. Comparative mutagenic effects of structurally similar flavonoids quercetin and taxifolin on tester strains *Salmonella typhimurium* TA102 and *Escherichia coli* WP-2 *uvrA*. *Environ. Mol. Mutagen.* **2009**, *50*, 451–459. [CrossRef]
54. Ono, K.; Nakane, H.; Fukushima, M.; Chermann, J.C.; Barre-Sinoussi, F. Differential inhibitory effects of various flavonoids on the activities of reverse transcriptase and cellular DNA and RNA polymerases. *Eur. J. Biochem.* **1990**, *190*, 469–476. [CrossRef]
55. Naki, A.; Varfolomeev, S.D. Mechanism of the inhibition of laccase activity from *Polyporus versicolor* by halide-ions. *Biochemistry* **1981**, *46*, 1344–1350. Available online: https://pubmed.ncbi.nlm.nih.gov/7295828/ (accessed on 30 March 2021).
56. Wu, B.-P.; Wen, Q.; Xu, H.; Yang, Z. Insights into the impact of deep eutectic solvents on horseradish peroxidase: Activity, stability and structure. *J. Mol. Catal. B Enzym.* **2014**, *101*, 101–107. [CrossRef]
57. Dai, Y.; Spronsen, J.; Witkamp, G.J.; Verpoorte, R.; Choi, Y. Natural deep eutectic solvents as new potential media for green technology . *Anal. Chim. Acta* **2013**, *766*, 61–68. [CrossRef] [PubMed]
58. Hammond, O.S.; Bowron, D.T.; Edler, K.J. The effect of water upon deep eutectic solvent nanostructure: An unusual transition from ionic mixture to aqueous solution. *Angew. Chem. Int.* **2017**, *56*, 9782–9785. [CrossRef] [PubMed]
59. Catauro, M.; Papale, F.; Bollino, F.; Piccolella, S.; Marciano, S.; Nocera, P.; Pacifico, S. Silica/quercetin sol-gel hybrids as antioxidant dental implant materials. *Sci. Technol. Adv. Mater.* **2015**, *16*, 035001. [CrossRef]
60. Zu, S.; Yang, L.; Huang, J.; Ma, C.; Wang, W.; Zhao, C.; Zu, Y. Micronization of taxifolin by supercritical antisolvent process and evaluation of radical scavenging activity. *Int. J. Mol. Sci.* **2012**, *13*, 8869–8881. [CrossRef]
61. Hasibi, F.; Nasirpour, A.; Varshosaz, J.; García-Manrique, P.; Blanco-López, M.; Gutiérrez, G.; Matos, M. Formulation and characterization of taxifolin-loaded lipid nanovesicles (liposomes, niosomes, and transfersomes) for beverage fortification. *Eur. J. Lipid Sci. Technol.* **2020**, *122*, 1900105–1900118. [CrossRef]

62. Heneczkowski, M.; Kopacz, M.; Nowak, D.; Kuźniar, A. Infrared spectrum analysis of some flavonoids. *Acta. Pol. Pharm.* **2001**, *58*, 415–420.
63. Bovey, F.A.; Mireau, P. *NMR of Polymers*, 1st ed.; Academic Press: London, UK, 1996; p. 459. ISBN 978-012-11-9765-0.
64. Kiehlmann, E.; Szczepina, M. Epimerization, transacylation and bromination of dihydroquercetin acetates; synthesis of 8-bromodihydroquercetin. *Cent. Eur. J. Chem.* **2011**, *9*, 492–498. [CrossRef]
65. Kiehlmann, E.; Slade, P. Methylation of dihydroquercetin acetates: Synthesis of 5-*o*-methyldihydroquercetin. *J. Nat. Prod.* **2003**, *66*, 1562–1566. [CrossRef]
66. Yamamura, S. Oxidation of phenols. In *PATAI'S Chemistry of Functional Groups*; Rapoport, Z., Ed.; John Wiley & Sons, Ltd: Hoboken, NJ, USA, 2003. [CrossRef]
67. Jones, S.; Solomon, E.I. Electron transfer and reaction mechanism of laccases. E. *Cell. Mol. Life Sci.* **2015**, *72*, 869–883. [CrossRef] [PubMed]
68. Smith, M.; March, J. *March's Advanced Organic Chemistry: Reactions, Mechanisms, and Structure*, 6th ed.; John Wiley & Sons: Hoboken, NJ, USA, 2007; 2357p, ISBN 978-047-17-2091-1.
69. Frisch, M.J.; Trucks, G.W.; Schlegel, H.B.; Scuseria, G.E.; Robb, A.M.; Cheeseman, J.R.; Scalmani, G.; Barone, V.; Petersson, G.A.; Janesko, B.G.; et al. *Gaussian 09, Revision A.02*; Gaussian, Inc.: Wallingford, CT, USA, 2009.
70. Prescott, A.; Stamford, N.; Wheeler, G.; Firmin, J.L. In vitro properties of a recombinant flavonol synthase from *Arabidopsis thaliana*. *Phytochemistry* **2002**, *60*, 589–593. [CrossRef]
71. Nifant'ev, E.; Mosyurov, S.; Kukhareva, T.; Vasyanina, L. Aminomethylation of Dihydroquercetin. *Dokl. Chem.* **2013**, *448*, 4–8. [CrossRef]
72. Boursalian, B.; Ham, W.; Mazzotti, A.; Ritte, T. Charge transfer directed radical substitution enables *para*-selective C–H functionalization. *Nat. Chem.* **2016**, *8*, 810–815. [CrossRef] [PubMed]
73. Gorshina, E.S.; Rusinova, T.V.; Biryukov, V.V.; Morozova, O.V.; Shleev, S.V.; Yaropolov, A.I. The dynamics of oxidase activity during cultivation of basidiomycetes from the genus *Trametes* Fr. *Appl. Biochem. Microbiol.* **2006**, *42*, 558–563. [CrossRef]
74. Ehresmann, B.; Imbault, P.; Well, J.H. Spectrophotometric determination of protein concentration in cell extracts containing tRNA's and rRNA's. *Anal. Biochem.* **1973**, *54*, 454–463. [CrossRef]
75. Chertkov, V.; Davydov, D.; Shestakova, A. Regioselective N-arylation of nitroazoles. Determination of the structure of N-arylnitroazoles on the basis of NMR spectroscopic data and quantum-chemical calculations. *Chem. Heterocycl. Compd.* **2011**, *47*, 45–54. [CrossRef]